CHAPTER 7

RESULTS AND DISCUSSION

7.1 Performance Metrics

The primary utilization of performance measures is to evaluate the efficacy of the proposed work which is elaborated in this section. The metrics used to evaluate proposed work are mentioned as follows,

- Accuracy
- Precision
- Recall
- F1 score

(i) Accuracy

Accuracy is the significant measure that is utilized to analyze the number of accurate predictions that are correct in the model. The accuracy formula is shown in equation Eq. (7.1).

$$Accu = \frac{TrN+TrP}{TrN+FlN+TrP+FlP} \quad (7.1)$$

Where TrP is True positive, TrN is True Negative, FlP is False Positive, and FlN is False Negative.

(ii) Precision

Precision is a measure to determine the number of positive predictions in the proposed model. It is computed to analyze the proposed model quality. The precision formula is defined in the Eq. (7.2),

$$Prec = \frac{TRP}{FLP+TRP} \quad (7.2)$$

(iii) Recall

The recall is a metric that is utilized to analyze the data percentage that is predicted appropriately in the model. The recall formula is represented in Eq. (7.3),

$$Re\_c = \frac{TRP}{FLN+TRP} \quad (7.3)$$

(iv) F1 score

F1-score is calculated to analyze the proposed model predictions based on positive class. The formula is depicted in Eq. (7.4),

$$F1 - score = 2 \times \frac{Rc \times Pc}{Rc + Pc} \quad (7.4)$$

Where Pc is the precision and Rc is the recall.

7.2 Environmental Configuration

The environmental setup incorporated in the proposed work to produce results is the Matlab 2022b simulation tool. Matlab's DNN tool has been employed for categorization. The CPU is an Intel ® core ™ i5 3210M with a 2.5 GHz CPU. The system inhibits 2GB RAM. Around 1883 sample images from two different datasets were considered for assessing the accuracy outcome of the proposed work.

Further, 70% of sample images are utilized for training and 30% of the sample images were considered for the validation process. The size of the trained images is 250 x 250 pixels, and these images are determined by the simulation outcome. Class labels are assigned to values in the hidden nodes depending on the features, and relevant values are mapped with the cervical cancer class label. Table 7.1 illustrates the system configuration for cervical cancer detection.

Table 7.1 System Configuration

Environment	Configuration
Software	Matlab 2022b
CPU	Intel ® core ™ i5 3210M
GPU	2.5 GHz
RAM	2 GB

7.3 Exploratory Data Analysis

The typical characteristics of EDA are to identify general patterns in the data that encompasses outliers and features of the data, which may be unexpected. Figure 7.1

showcases the sample cells of the SIPAKMED dataset, comprise of cells including Superficial Intermediate, Koilocytotic, Parabasal, Dyskeratotic, and Metaplastic.

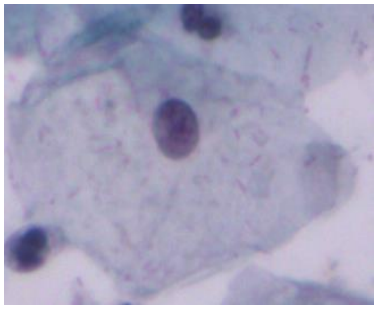

(a)Superficial Intermediate (Normal)

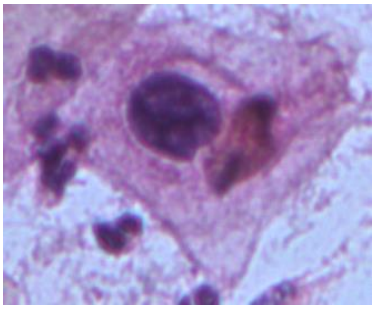

(b)Koilocytotic (Pre-cancerous)

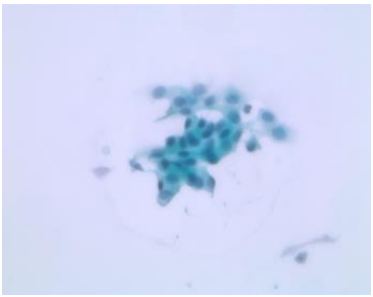

(c)Parabasal (Normal)

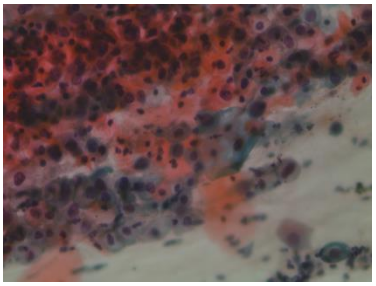

(d)Dyskeratotic(Pre-cancerous)

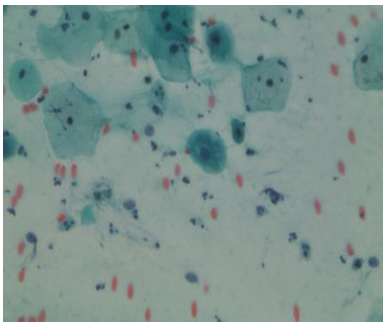

(e)Metaplastic (Cancerous)

Figure 7.1 Cells of SIPAKMED Dataset

Figure 7.1 depicts the samples of the SIPAKMED dataset for multiclass classification of cervical cancer cells. Superficial intermediate cells are normal cells in accordance with cervical cell classification. Koilocytotic cells refer to the cellular changes characterized by wrinkled nuclei, hyperchromasia, binucleation, or multinucleation often related to HPV infections; Parabasal cells includes hyperplasia with minimal nuclear atypia in the basal layer, which indicates pre-cancerous changes. Dyskeratotic exhibits abnormal maturation and proliferation with features including nuclear enlargement and irregular nuclear membranes,

and eventually, metaplastic displays different conditions such as atrophy, immature metaplasia, and other conditions

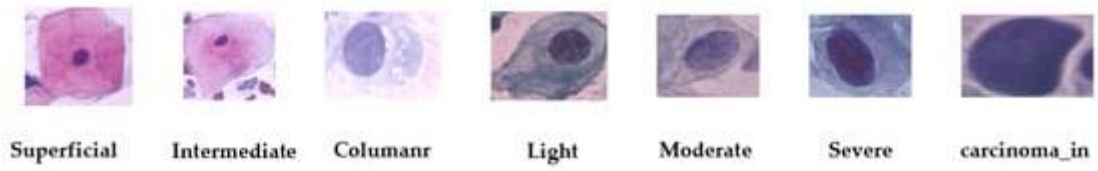

Figure 7.2 Herlev dataset sample

From the figure 7.2, it can be identified that, Herlev dataset samples encompasses of different cells with the constraint of considering superficial, Intermediate and columnar cells as normal. In addition, Light, Moderate and Severe are known to be pre-cancerous and Carcinoma_in_situ are known to be cancerous cells.

The subsequent section deals with the experimental outcome obtained by the proposed models using two different datasets.

7.4 Experimental Outcomes

This section shows the experimental outcome obtained by the proposed models for the effective classification of cervical cancer cells. As mentioned above, from cervical cancer images in SIPAKMED dataset and Herlev dataset, 70% of the images in both the datasets were taken for training whereas 30% of the images were used for testing.

7.4.1 Model 1 (CERVI-CYTO-NET)

Single Cell Image Results

Results obtained for single cell using CERVI-CYTO-NET is displayed in Figure 7.3.

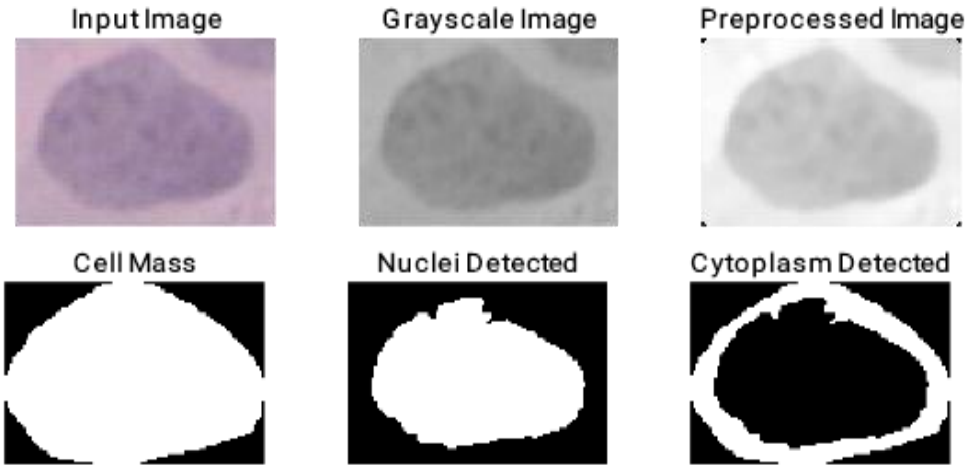

Figure 7.3 Segmentation for single cell

Figure 7.3 depicts the segmentation process carried out for single cell classification using CERVI-CYTO-NET, where the process is performed by feeding the input image to the model, then converting it to grayscale image and subsequently pre-process the image accordingly. Figure 7.4 depicts the classification result for single cell image using Model 1.

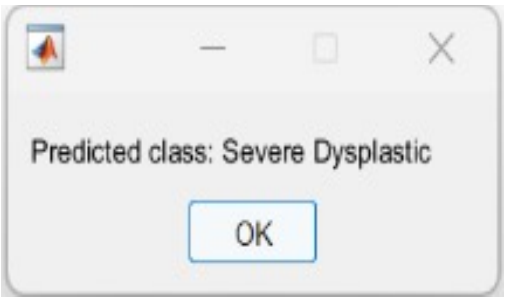

Figure 7.4 Classification outcome for single cell

Multi-Cell Image Results

Similarly, the outcome obtained from multi cell classification using CERVI-CYTO-NET is explained in the subsequent section and in Figure 7.5. Here, the process is performed by passing the input image to the model, then converting the image to gray scale and then the image is pre-processed, where nuclei and cytoplasm is detected.

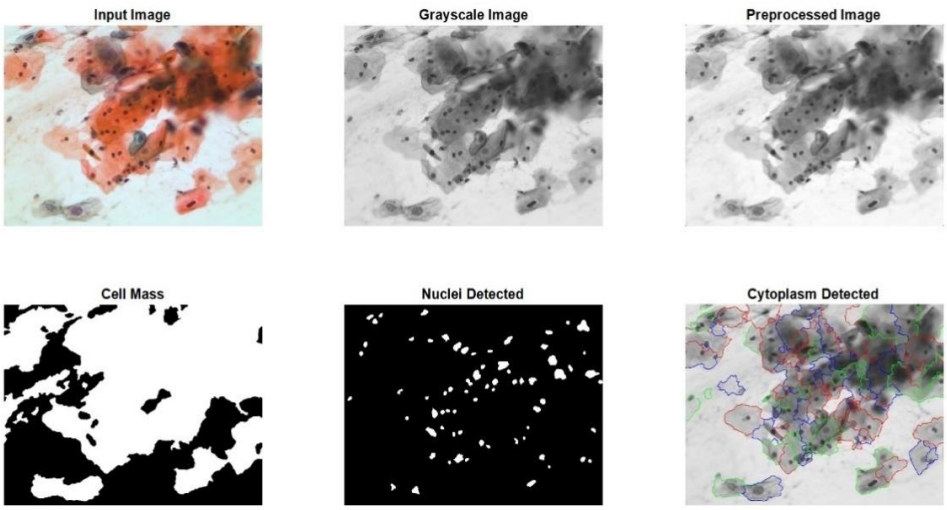

Figure 7.5 Multi cell Segmentation for Model 1

Eventually, following the segmentation process, classification is performed through incorporating the proposed RV-DLNN model. In this model, the cervical cancer cells

classification is performed, and the type of cancer cell obtained by the proposed model is depicted in the text box, as illustrated in Figure 7.6.

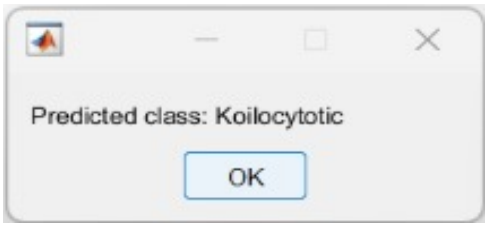

Figure 7.6 Classification outcome for Model 1

7.4.2. Model 2 (CERVI-CYTO-RBM)

Segmented images for single cell and multi cell classification are displayed in Figure 7.7 and Figure 7.8.

Single cell Image Results

Figure 7.7 shows the involving procedure in single cell classification through improved weighted FCM process.

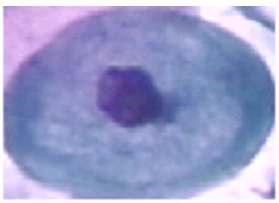

Input Image

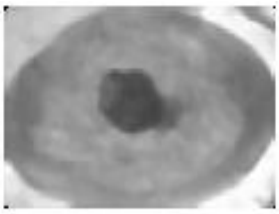

After ADF with HE

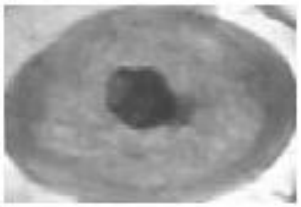

Filtered Image

Segmentation with improved weighted FCM

Figure 7.7 Single cell segmentation for Model 2

Where the process is implemented by sending the input image, after that ADF with HE is processed and then image is filtered and eventually segmented image is obtained. Similar to single cell classification, multi cell classification is also depicted in upcoming section.

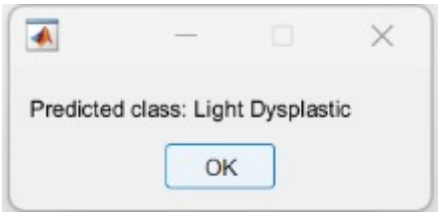

Figure 7.8 Classification result for Model 2

Multi-cell Image Results

Corresponding to Model 1, Model 2 concentrates on the cervical cancer cells classification for multi cell. Figure 7.9 shows the input image utilized for multi cell classification, and in Figure 7.10, the conversion of RGB to grayscale is illustrated.

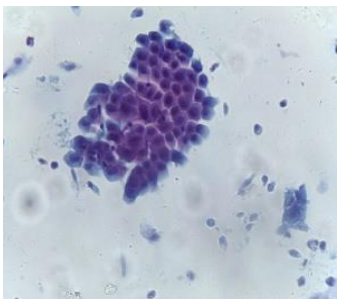

Figure 7.9 Input image

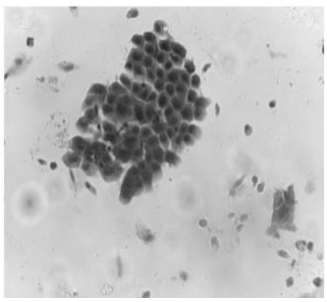

Figure 7.10 Conversion of RGB to Grayscale

In Figure 7.10, the conversion of RGB to grayscale is performed to achieve a simplified image analysis, thereby aiding the proposed model in detecting abnormalities and classifying the cancer cells precisely. Grayscale images comprise only shades of gray representing the luminous intensity of the images and facilitates in highlighting structural details and abnormalities in the cells unaccompanied by the complexity of color information. This conversion of RGB to grayscale also plays a crucial role in cervical cancer screening allowing better segmentation of images. The filtered images are shown in Figure 7.11 and Figure 7.12

Figure 7.11 Filtered Image

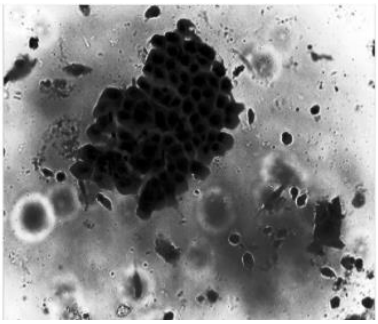

Figure 7.12 ADF with HE (After)

Subsequently the grayscale images are prompted for performing filtering and pre-processing techniques such as ADF with HE is implemented. The hybridization ADF with HE focuses on minimizing the disorder without removing the edges and enhances the image contrasts for an improved segmentation.

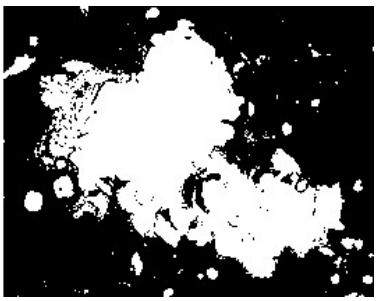

Figure 7.13 Segmentation using improved-weighted FCM

Figure 7.13 depicts the segmentation process involved using the proposed i-WFCM model. i-WFCM, employed for cervical cancer cell classification, determines the cluster center of an image in the process of segmentation; thereby an effective feature is successfully extracted. Eventually, the RBM-DBN classifier was implemented for cancer cells classification, in which the output depicted in Figure 7.14, illustrates the predicted type of

cancer cell as Superficial Intermediate obtained by the proposed model II for the cervical cancer cells classification.

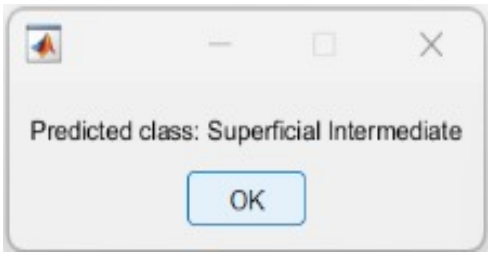

Figure 7.14 Cancer cell classification

7.4.3. Model 3 (CERVI-CYTO-CNN)

Model 3 is also capable of signifying both single cell and multi-cell classification of cervical cancer. Thus, each subsection of Model 3 displays both single cell and multi-cell classification.

Single cell Image Results

The process involved in single cell image classification is depicted as follows. The original test RGB image is showed initially in Figure 7.15.

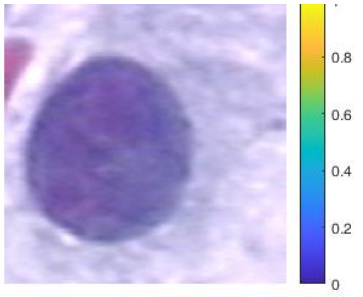

Figure 7.15 Original Test RGB image

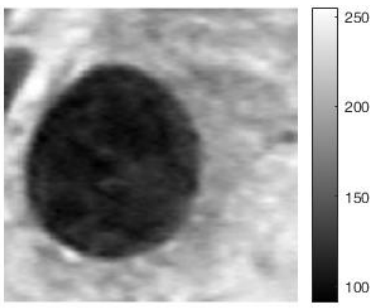

Figure 7.16 Grayscale image

Figure 7.15 and Figure 7.16 illustrates the RGB test image and grayscale test image obtained for single cell classification using Model 3.

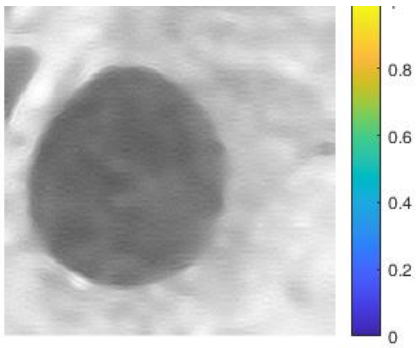

Figure 7.17 Preprocessed Using ADF with Dragonfly Optimization

After converting images from RGB to grayscale, pre-processing is incorporated by combining ADF and Dragonfly optimization technique and is depicted in Figure 7.17. Incorporating the combined ADF and Dragonfly technique helps reduce the noise present in the image. Figure 7.18 shows the segmented image for a single cell using segmentation technique and Figure 7.19 illustrates the result obtained for segmentation process.

Figure 7.18 Segmented image

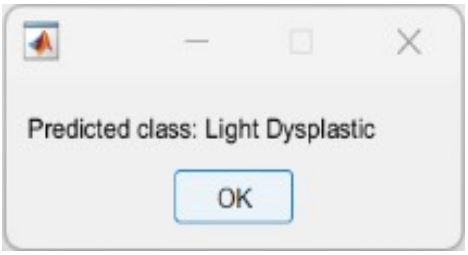

Figure 7.19 Classification Result

Multi-cell Image Results

Identical to single cell classification, multi-cell classification involving similar steps, including RGB conversion to grayscale, are highlighted in Figures 7.20 and 7.21.

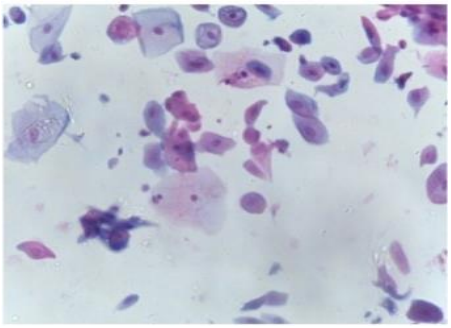

Figure 7.20 Input Image

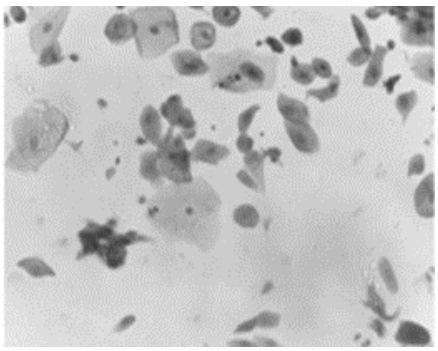

Figure 7.21 Conversion of RGB to Grayscale

After converting RGB to grayscale, pre-processing is incorporated using combined ADF and Dragonfly optimization technique. Similar to the process involved in single cell classification, multi-cell classification applied similar technique for effective pre-processing of data, and the preprocessed image is depicted in Figure 7.22.

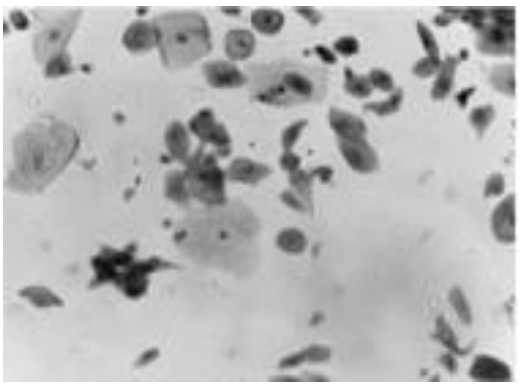

Figure 7.22 Pre-processing using ADF with DO

Figure 7.23 depicts the test function and the convergence curve. The convergence curve visualizes the enhancement of the algorithm over time, especially for optimization algorithms. Convergence curves are important for gauging the rate at which the algorithms converge towards the solution.

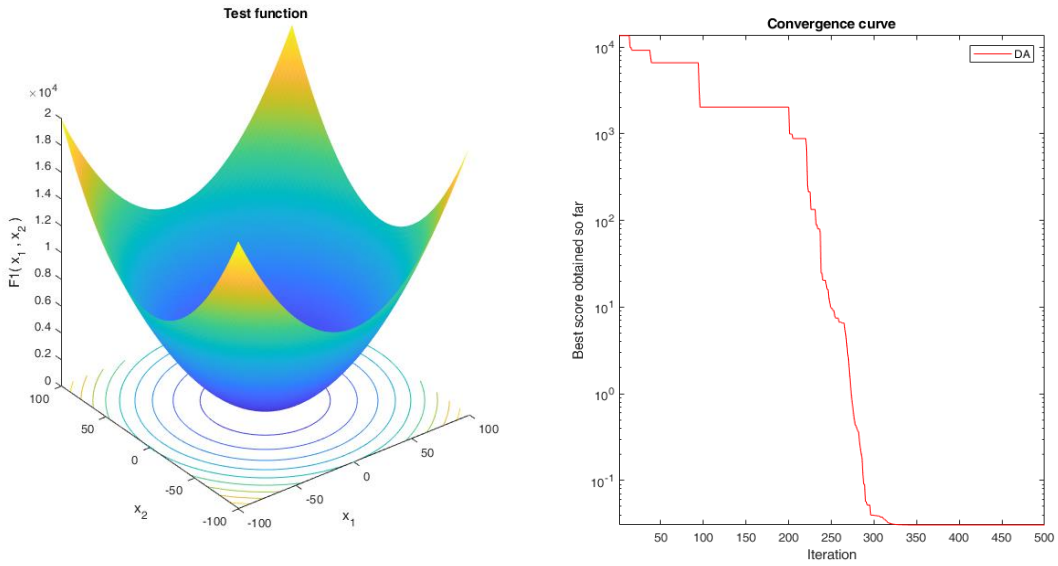

Figure 7.23 Convergence plot and test function using ADF with DO

After pre-processing, segmentation is executed where i-WFCM-GOA algorithm is utilized in the proposed method to raise the weighted factor for the clustering center without making computation more difficult.

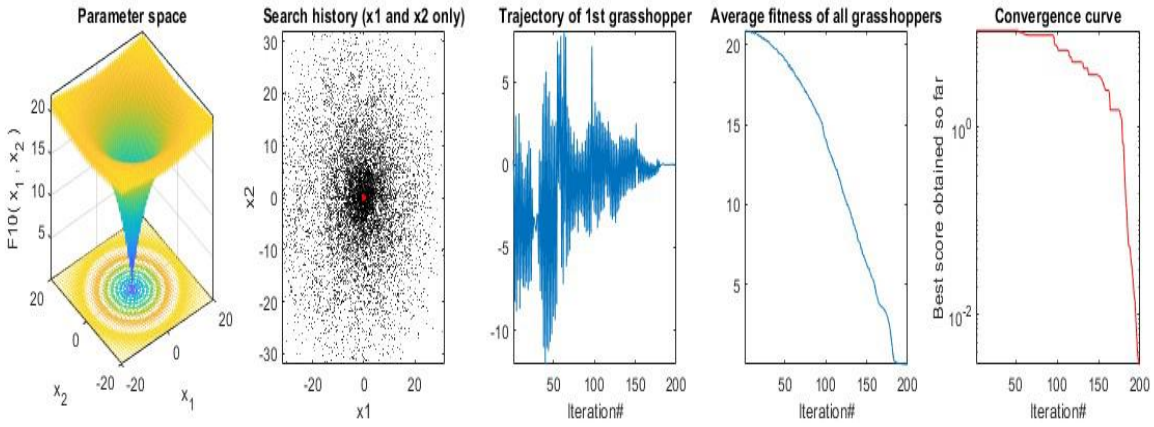

Figure 7.24 Grasshopper Optimization Algorithm for Segmentation

Thus, figure 7.24 shows the search history, trajectory of 1st grasshopper, parameter space, convergence curve and average fitness of all grasshoppers. Subsequently, the

segmented images of multi-cells through improved - weighted FCM with GOA for optimization are highlighted in Figure 7.25.

Figure 7.25 improved-Weighted FCM with GOA for Optimization

Figure 7.26 illustrates the classification of predicted cancer cells using the proposed DCNN method for multi-cell classification.

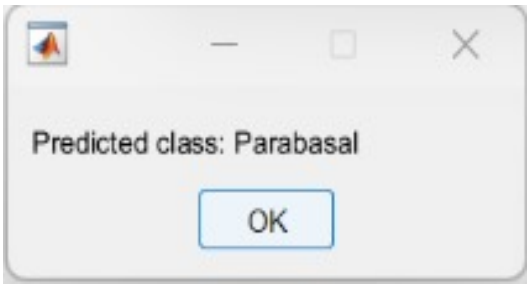

Figure 7.26 Multi-cell classification

In addition to these outcomes obtained by the model, the efficacy of the proposed work needs to be assessed to better analyze the model's performance. Thus, the following section deals with evaluating the proposed model by incorporating diverse evaluation metrics involving accuracy, precision, recall rate, F1- score and confusion matrix.

7.5. Performance Analysis

The proposed method's performance is analyzed using evaluation metrics such as accuracy, precision, recall, and F1-score. Furthermore, the Confusion Matrix is applied to identify the proposed model's performance. It envisages and encapsulates the classification algorithm's performance.

The proposed RVDLNN is evaluated using various performance metrics, such as accuracy, precision, recall and F1 Score. Table 7.2 describes the proposed RVDLNN metrics and their values.

Table 7.2 Performance Analysis for CERVI-CYTO-NET

Metrics	Single cell	Multi cell
Accuracy (%)	92.73	93.08
Precision (%)	71.15	82.61
Recall (%)	88.10	87.69
F1 score (%)	78.12	85.07

The above table demonstrates the metric values for both single cell and multi cell classification, in which accuracy, precision, recall and F1 score are achieved by model I for single cell classification is 92.73%, 71.15%, 88.10% and 78.12%. On contrast, accuracy, precision, recall and F1 score attained for multi cell is 93.08%, 82.61%, 87.69% and 85.07%. Graphical representation of Table is denoted in Figure 7.27.

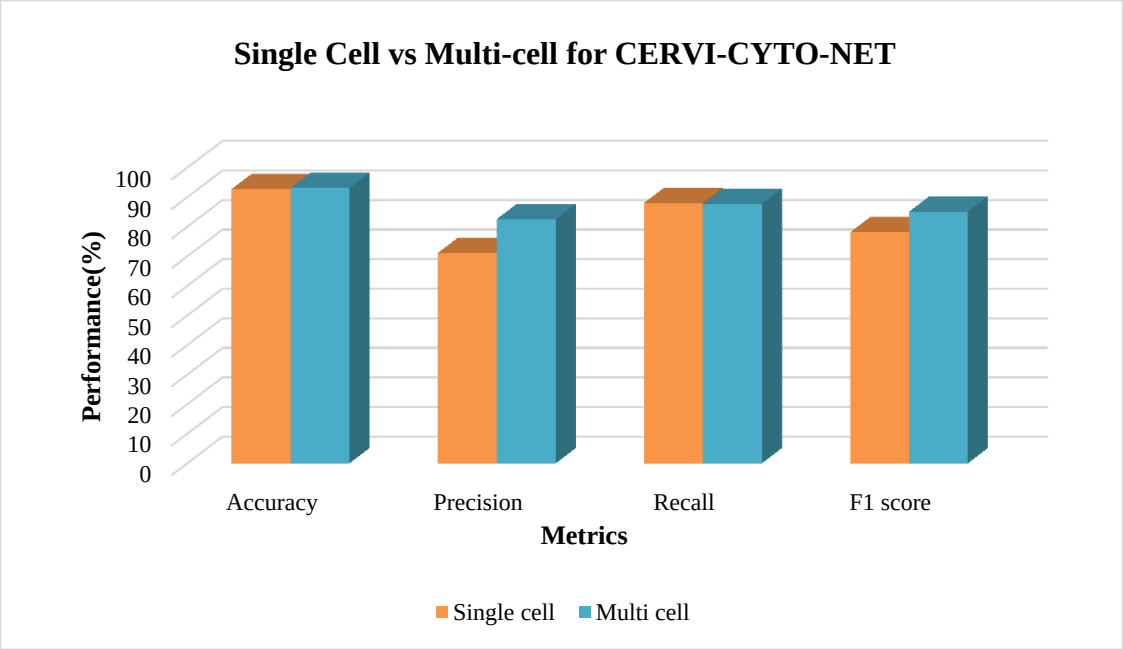

Figure 7.27 Performance Analysis of CERVI-CYTO-NET

Figure 7.27 signifies the performance metrics of the proposed RVDLNN model in terms of accuracy, precision, recall and F1 score. In addition, confusion matrix for both single cell and multi cell for model I is illustrated in Figure 7.28 (a) and Figure 7.28 (b).

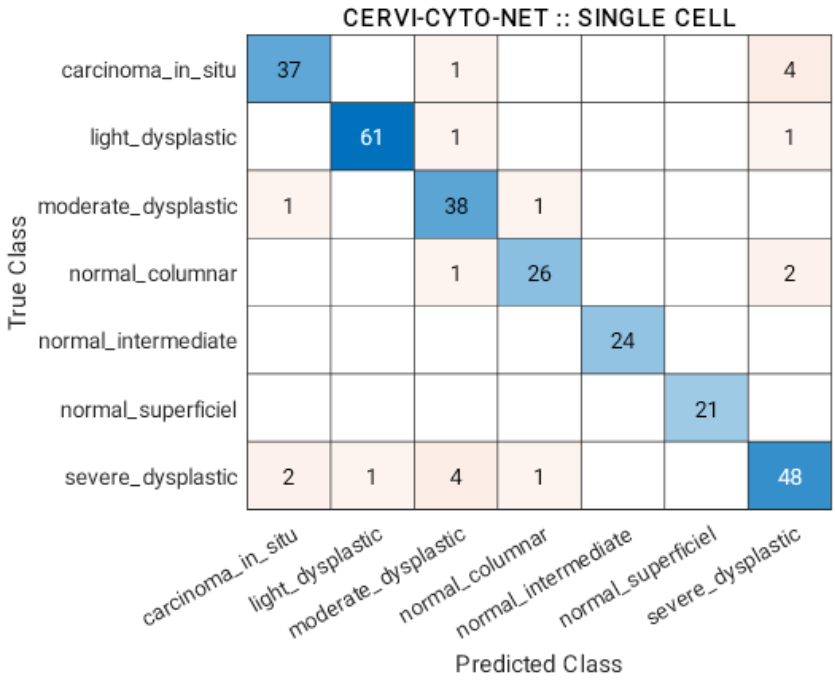

Figure 7.28 (a) Confusion Matrix for single cell classification using Model 1

Figure 7.28 (a) and Figure 7.28 (b) shows the confusion matrix for Model 1, in which diagonal elements show the number of instances that were accurately classified in each class and the off-diagonal elements depicts the number of misclassified instances. The proposed method is responsible for identifying both single cell and multi cell classification, where number of correct classifications is higher and better compared to misclassification.

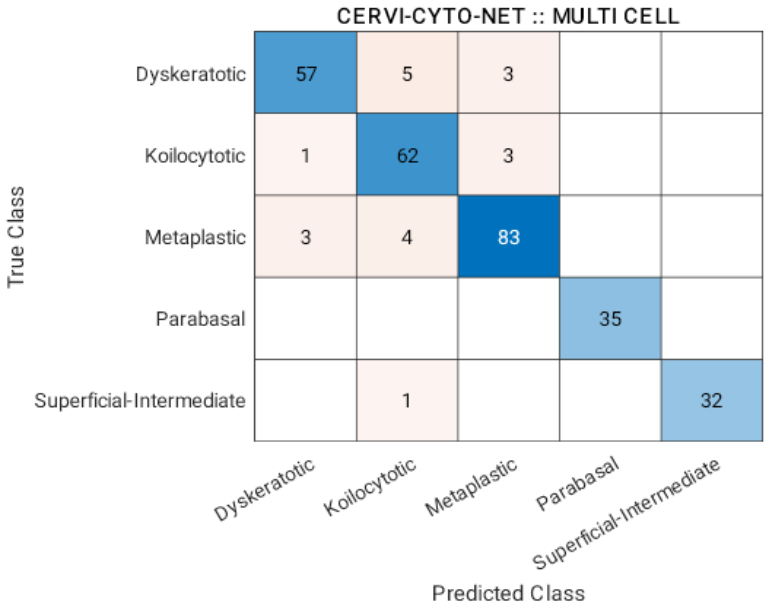

Figure 7.28 (b) Confusion Matrix for multi cell classification using Model 1

Additionally, the Table 7.3 illustrates the performance measures of the proposed RBM-DBN. In each iteration, a number of image datasets is raised for successfully testing and evaluated using performance metrics including Accuracy, precision, recall, and F1-score.

Table 7.3 Performance analysis of CERVI-CYTO-RBM

Metrics	Single cell	Multi cell
Accuracy	95.27	93.08
Recall	79.59	87.69
Precision	92.86	82.61
F1-score	89.71	85.07

The table describes metric value obtained for single cell and multi cell for Model 2, in which accuracy gained for single cell classification, is 95.27%. Meanwhile, recall, precision and F1 score attained for single cell is 79.59%, 92.86% and 89.71%. Correspondingly, for multi cell the performance is achieved in terms of accuracy, recall, precision and F1 score are 93.08%, 87.69%, 82.61% and 85.07%. Illustrative exemplification of single cell vs multi cell for CERVI-CYTO-RBM is denoted in Figure 7.29.

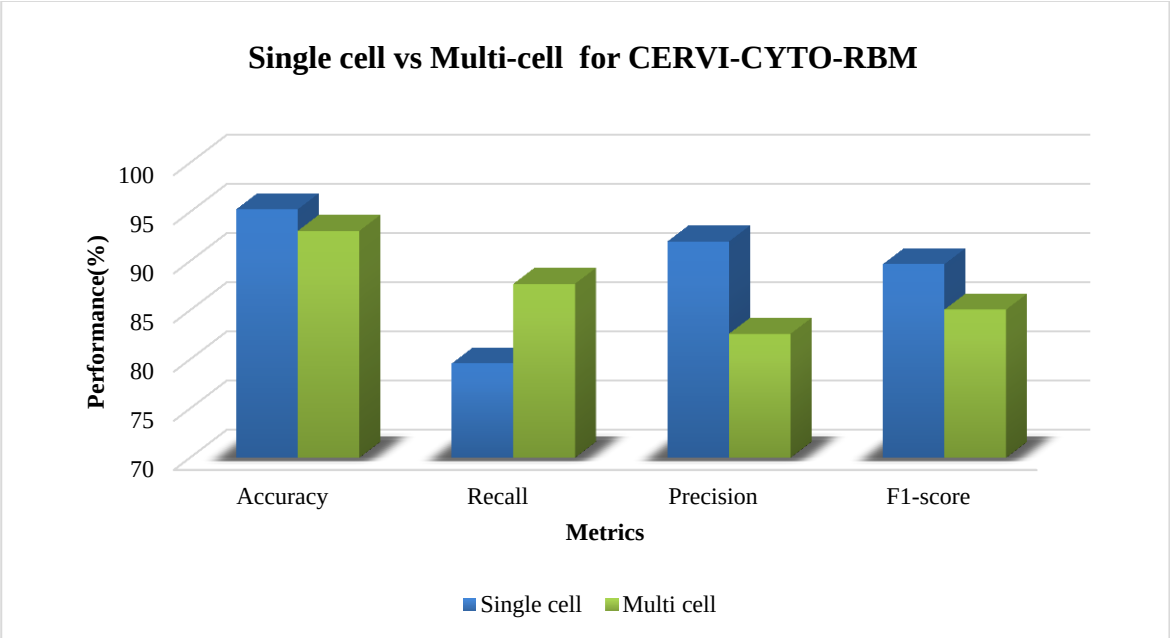

Figure 7.29 Performance Analysis of Proposed CERVI-CYTO-RBM

Figure 7.29 shows that the proposed RBM-DBN attained better results in performance metrics, which describes the efficiency of the RBM-DBN model for both single cell and multi cell classification. Figure 7.30 (a) and Figure 7.30 (b) showcases the confusion matrix for CERVI-CYTO-RBM model for single cell and multi-cell.

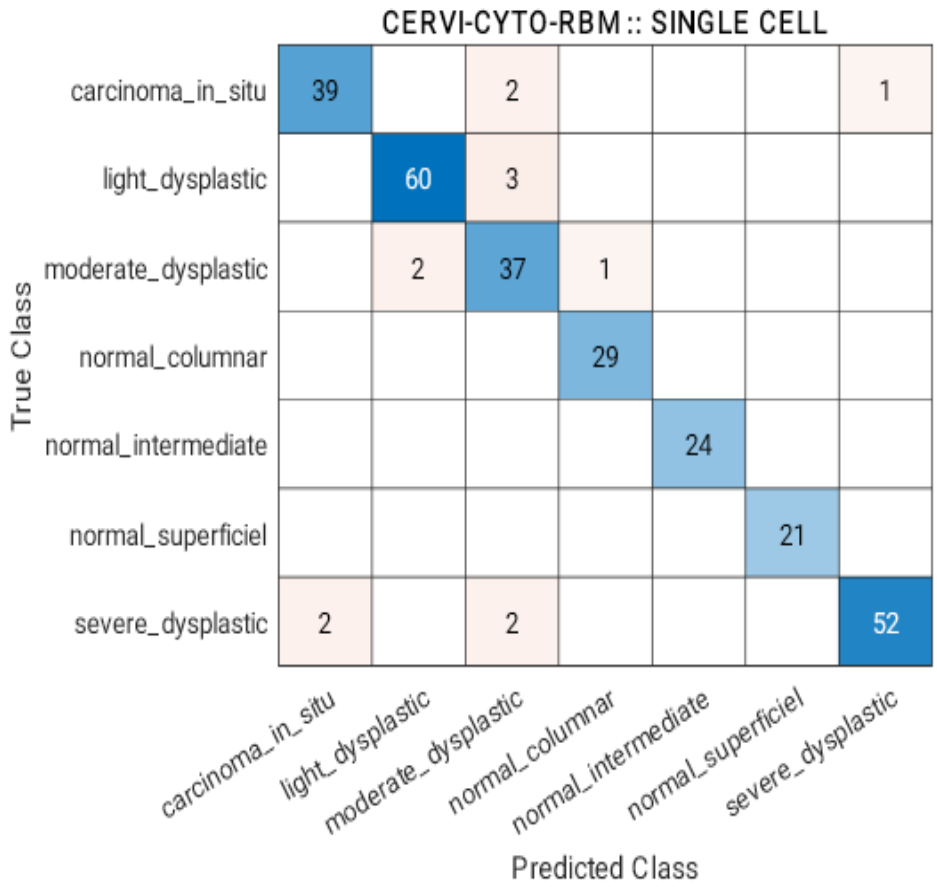

Figure 7.30 (a) Confusion matrix for Single cell classification using Model 2

From Figure 7.30 (a) and Figure 7.30(b), it is perceived that proposed Model 2 offers better result for single cell classification and multi cell classification where it exhibits higher values along the diagonal, indicating accurate and effective prediction. Further, in figure, the highest accurate prediction is obtained for class light_dysplastic followed by severe_dysplastic for Herlev dataset and for multiclass classification, highest accurate prediction is obtained for class Metaplastic.

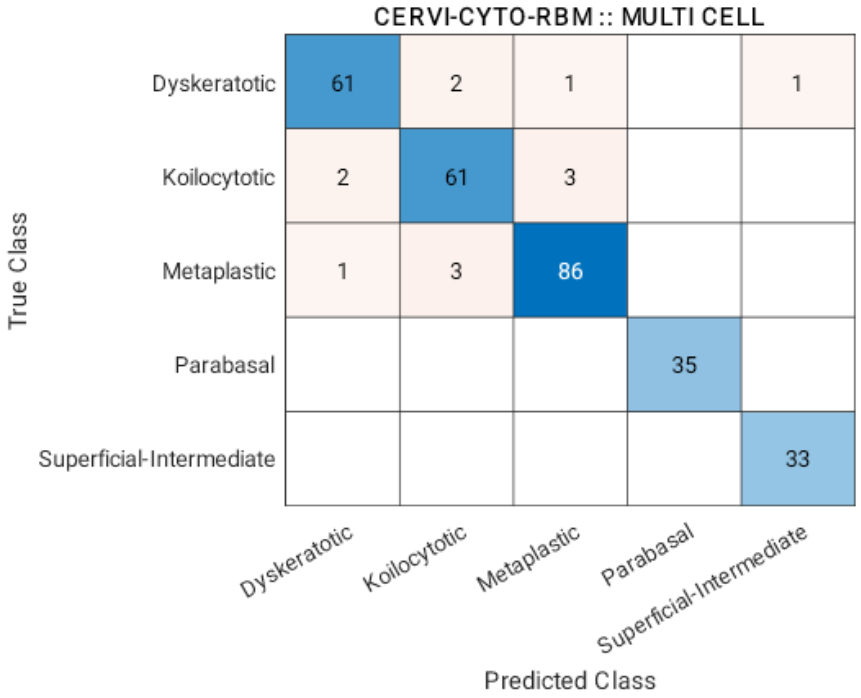

Figure 7.30 (b) Confusion matrix for Multi cell classification using Model 2

Similarly, the performance analysis of proposed DCNN in model 2 for single cell classification illustrated in table 7.4 exemplifies the proposed DCNN with ReLU for a single cell classification of cervical cancer.

Table 7.4 CERVI-CYTO-CNN results for Single Cell

Metrics	**Performance (%)**
Accuracy	96.73
Recall	95.24
precision	85.11
F1 score	89.89

The table shown above signifies the performance of proposed DCNN with ReLU for a single cell classification of cervical cancer. It accomplished 96.73% of accuracy, 95.24% of recall, 85.11% of precision and 89.89% of F1 score. In addition, the figure 7.31 shows the Performance Metrics of Single cell.

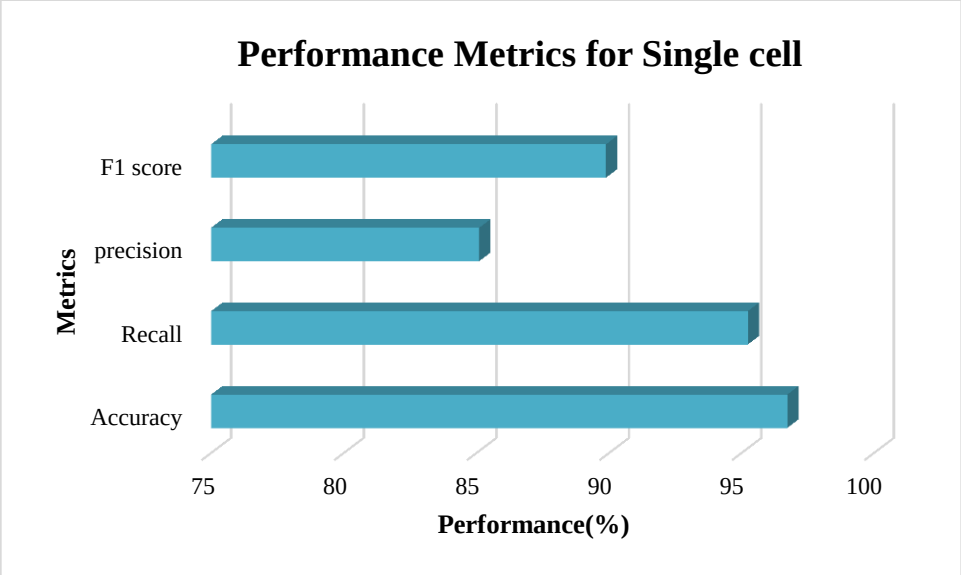

Figure 7.31 Performance Metrics of Singlecell

Figure 7.31 deliberates the performance metrics of the proposed DCNN with ReLU for a single cell classification. Figure 7.32 depicts the model accuracy of the proposed DCNN with ReLU for a single cell classification.

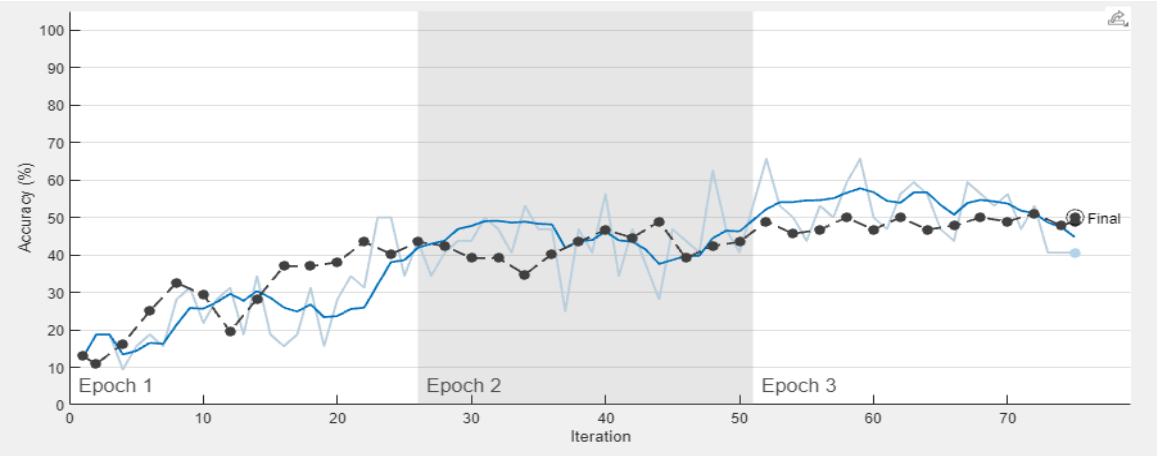

Figure 7.32 Model Accuracy of CERVI-CYTO-CNN for single cell

Figure 7.32 clearly depicts the performance of model for the proposed DCNN-ReLU algorithm in each iteration based on accuracy. The classifier's performance is assessed utilizing the accuracy when the loss function is incorporated to optimize and improve the overall performance. Figure 7.33 depicts the model loss function i.e., the frequency of error in the proposed DCNN technique with ReLU.

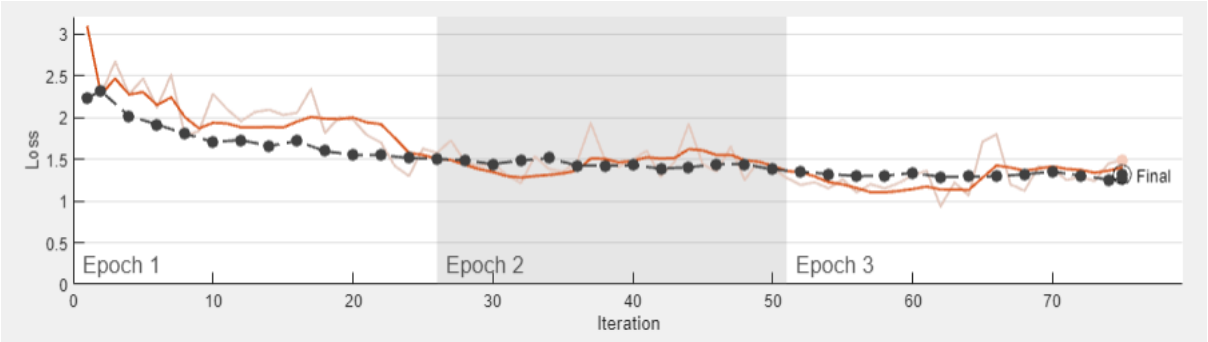

Figure 7.33 Model Loss Function of CERVI-CYTO-CNN for Single Cell classification

Figure 7.33 shows that loss function is reduced to enhance the performance of the proposed DCNN model. In proposed DCNN model, as iteration and accuracy increases, the loss function decreases. The figure signifies that the loss function decreases at iteration 2. Moreover, Figure 7.34 shows the performance evaluation of the proposed DCNN model.

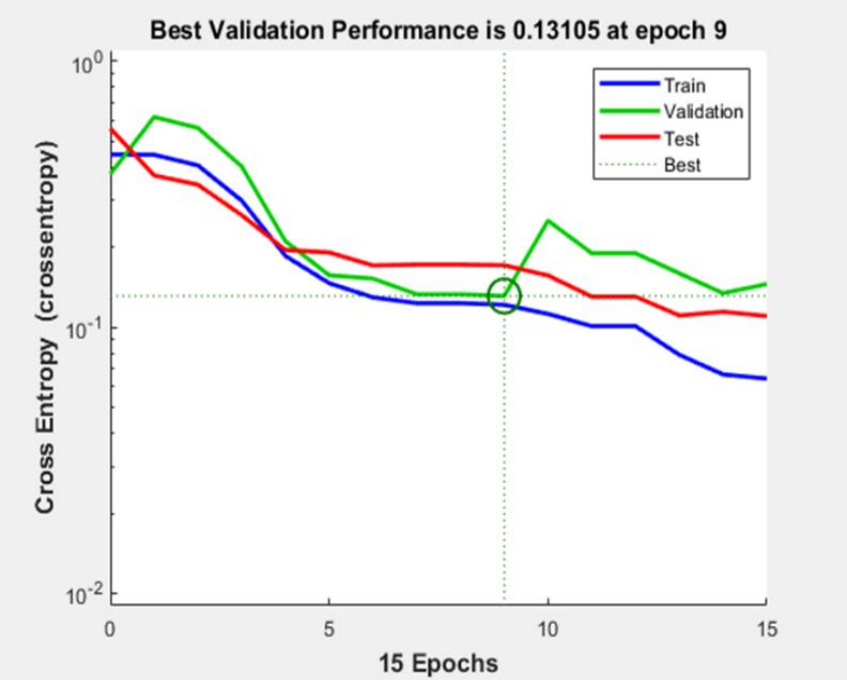

Figure 7.34 Performance evaluation of CERVI-CYTO-CNN for Single Cell classification using Cross Entropy

Figure 7.34 represents the performance assessment of the proposed DCNN-ReLUby cross entropy with 15 epochs. The best performance is achieved at epoch 9, with a value of 0.13105. Figure 7.35 shows the Confusion matrix of the proposed DCNN-ReLU for cervical cancer classification using single cell.

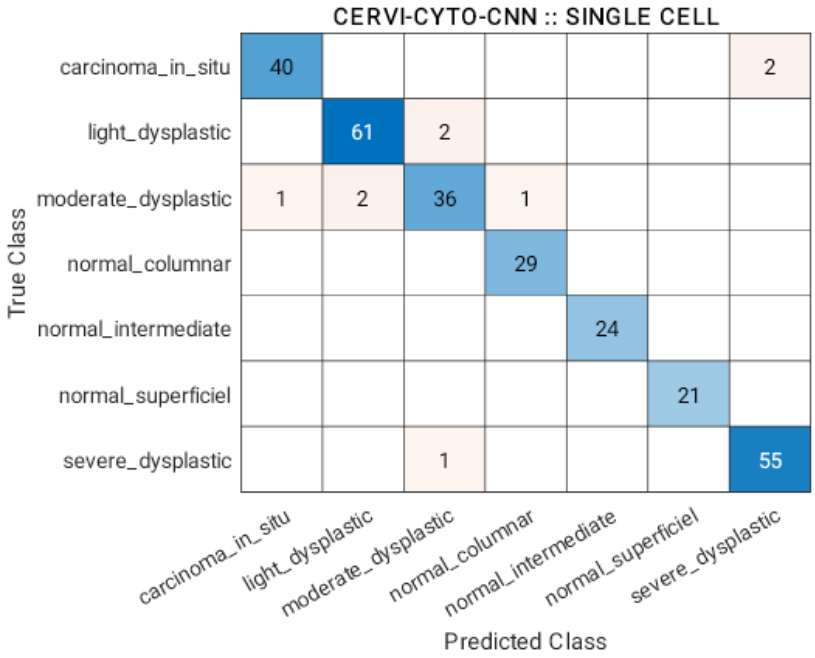

Figure 7.35 Confusion Matrix for single cell classification using Model 3

Figure 7.35 signifies the outcome of confusion matrix for the proposed DCNN-ReLU model in single cell classification. Basically, the confusion matrix represents the true positive, false positive, true negative and false negative values. In the matrix, outcome is analyzed based on actual value and predicted value. It can be seen from the above figure, that the proposed DCNN-ReLU model made the appropriate prediction with less error values. Thus, the proposed DCNN-ReLU effectively identifies the CC without any errors; hence, the proposed model is considered an error prone model.

Table 7.5 depicts the performance analysis of the proposed DCNN-ReLU for multi-cell classification of cervical cancer.

Table 7.5 Performance analysis of CERVI-CYTO-CNN for Multi-Cell

Metrics	Performance %
Accuracy	97.23
Recall	96.92
Precision	91.30
F1 score	94.03

The above table illustrates that the proposed DCNN-ReLU attained 97.23% of accuracy, 96.92% of Recall, 91.30% of precision and 94.03% of F1 score. Figure 7.36 deliberates the proposed model classification performance for classifying cervical cancer using multi-cell.

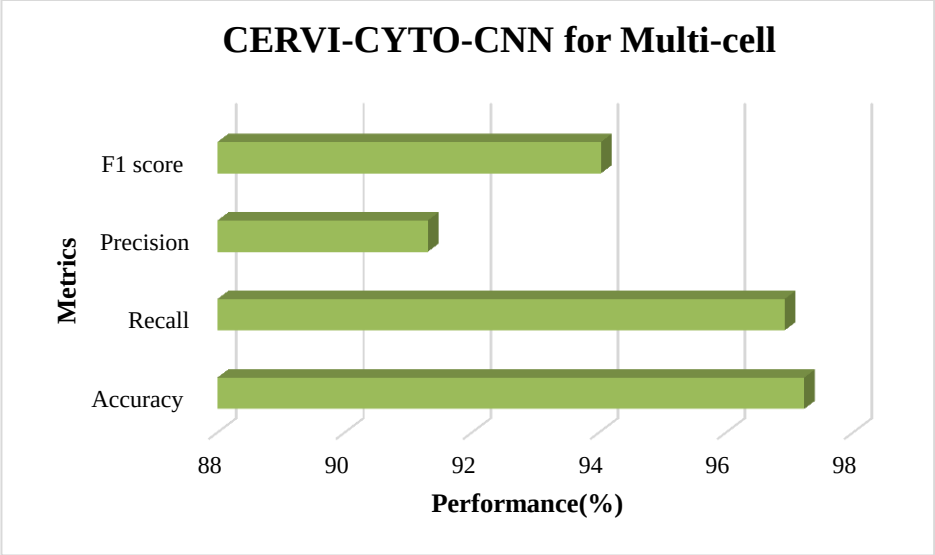

Figure 7.36 Performance Analysis of CERVI-CYTO-CNN for Multi-cell

Above figure shows the performance of proposed DCNN-ReLU technique which is analyzed on the basis of F1 score, recall, precision and accuracy for cervical cancer classification utilizing multi cell images. It attains better results, which shows the proposed model's performance.

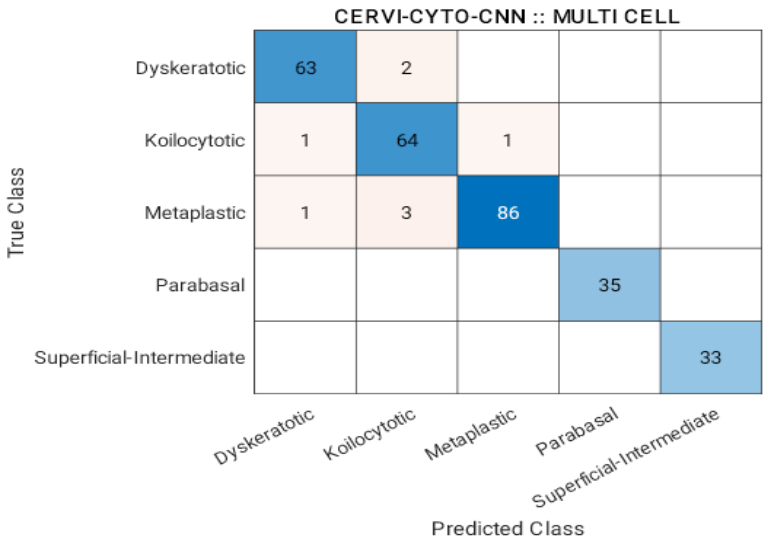

Figure 7.37 Confusion Matrix for Multi-cell classification using Model 3

Figure 7.37 deliberates the confusion matrix of the proposed DCNN-ReLU for Multi-cell. It shows the true class and predicted class for the multi-cell.

7.6. Comparative Analysis

The performance comparison of the proposed model in terms of accuracy, precision, recall and f-score measures, illustrate the efficiency of the proposed model for classifying cells of cervical cancer. Numerous mechanisms and algorithms were utilized through the existing models and produced outcomes. Hence, the attained results are compared with the proposed models. Various conventional models of DLNN, AlexNet and ResNet50v2 are represented in Table 7.6.

7.6.1. Model 1

Table 7.6 Comparison Results of RVDLNN(CERVI-CYTO-NET)

Methods	Accuracy (%)	Precision (%)	Recall (%)	F-measure (%)
DLNN	92.5	85	84	80
AlexNet	92	86	83	80
ResNet50V2	90	84	80	79.5
RVDLNN (CERVI-CYTO-NET)	93.08	82.61	87.69	85.07

Above table illustrates the comparative analysis of the proposed RVDLNN model where the performance is compared with other conventional models in terms of above-mentioned performance metrics. The proposed RVDLNN achieved 93.08% accuracy, 82.61% precision, 87.69% recall, and 85.07% F-measure. Since the proposed model using RVDLNN attained higher values than the existing models, it shows efficiency. Figure 7.38 deliberates the classifier performance of the proposed RVDLNN model.

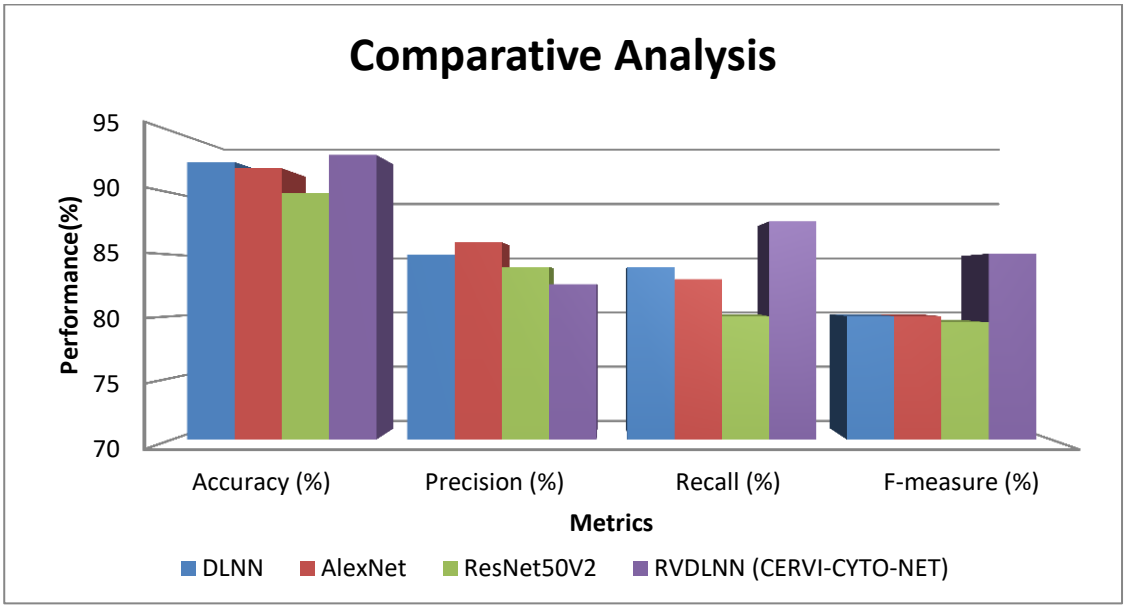

Figure 7.38 Classifier Performance

The Figure shows that the proposed model RVDLNN attained higher values compared to conventional model by attaining 0.57% accuracy, and 3.69% Recall and 5.07% F-measure, more than the conventional DLNN, AlexNet, and ResNet50V2 models.

7.6.2. Model 2

Table 7.7 shows the comparison of training accuracy and testing accuracy of the proposed RBM-DBN model with other conventional models.

Table 7.7 Comparison of Training Accuracy and Testing Accuracy of RBM-DBN (CERVI-CYTO-RBM)

Models	Train loss	Test loss	Training accuracy	Testing accuracy
ResNet50V2	0.730	0.270	0.899	0.900
AlexNet	0.241	0.235	0.912	0.925
DLNN	0.305	0.368	0.912	0.920
RVDLNN (CERVI-CYTO-NET)	0.191	0.191	0.842	0.935
RBM-DBN (CERVI-CYTO-RBM)	0.125	0.126	0.921	0.946

The above table deliberates the comparison of the proposed RBM-DBN model's training and testing with other conventional models. The proposed RBM-DBN model attained minimal loss with maximum accuracy than other conventional models, which shows the efficiency of the proposed model's performance.

Correspondingly, Table 7.8 depicts the outcomes of the classifiers.

Table 7.8 Overall Performance for Cancer Identification

Methods	Accuracy %	Precision %	Recall %	F1 score %
ResNet50V2	90	72.3	70.5	73.5
AlexNet	92	78.4	72	74
DLNN	92.3	78.6	73	75.5
CERVI-CYTO-NET	93.08	82.61	87.69	85.07
DBN	95	82.5	76.5	79
CERVI-CYTO-RBM	95.50	87.14	93.85	85.07

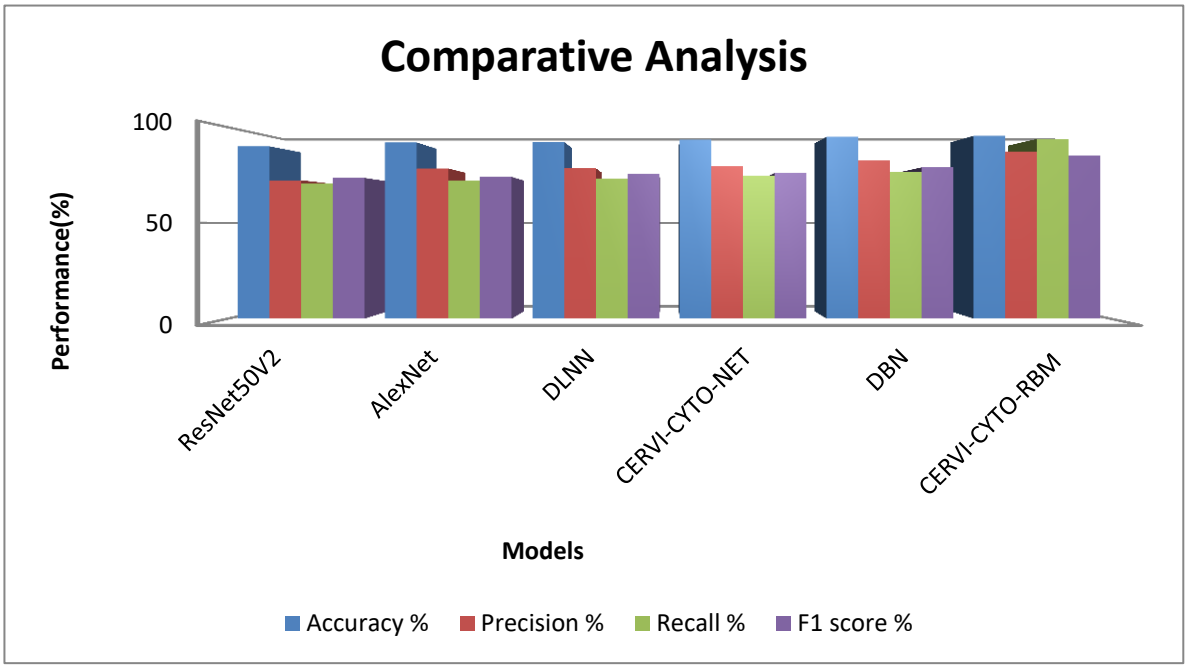

Figure 7.39 Overall Performance of Cancer Classification

Table 7.8 depicts that the proposed method outperformed other conventional classifiers involving ResNet50V2, AlexNet, DLNN, RVDLNN, and DBM. The proposed RBM-DBN obtained 95.50% accuracy, 88.61% Precision, 97.69% Recall, and 85.07% of F1 score which is higher compared to other existing models. Figure 7.39 represents the overall performance of cancer classification.

The acquired results are crucial when it is compared with the existing models because the higher accuracy is achieved with the similar type of dataset i.e., 95.3% accuracy. The proposed RBM-DBN is precise and quick which helps in attaining accuracy of this range.

7.6.3. Model 3

Figure 7.40 deliberates the Computational time of above mentioned classifiers for cervical cancer classification using model III.

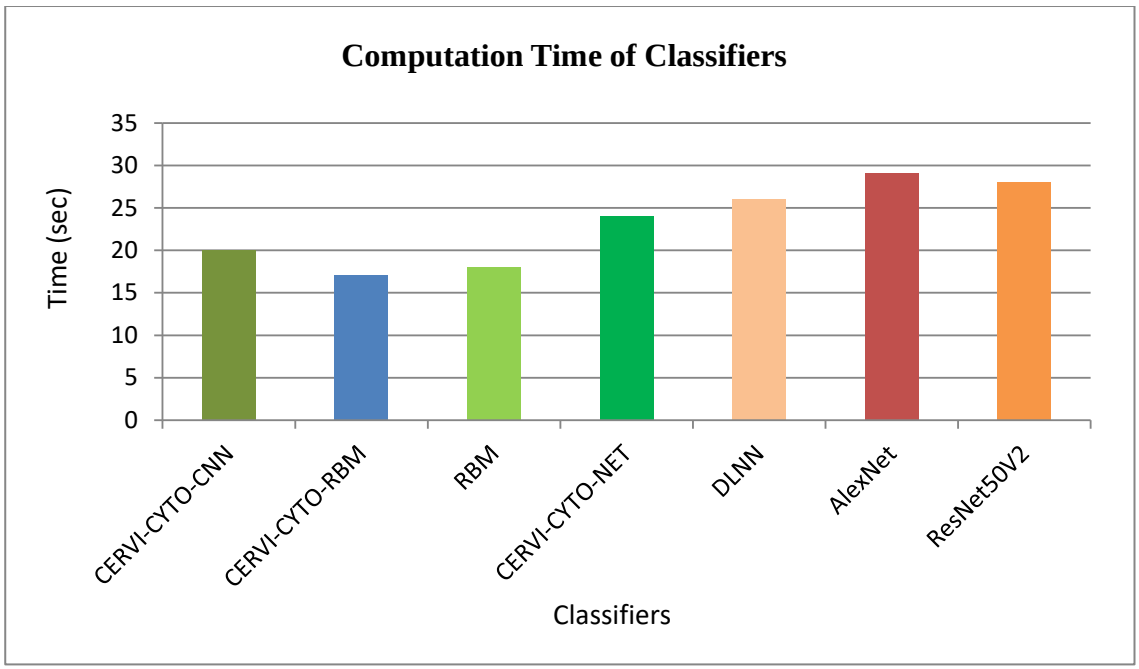

Figure 7.40 Computational Time of Classifiers

The computational time of classifiers depicted in Figure 7.40 is required by different models including ResNet50V2, AlexNet, DLNN, CERVI-CYTO-NET, RBM, CERVI-CYTO-RBM, and CERVI-CYTO-CNN. The proposed CERVI-CYTO-RBM obtained less computational time than others. Though it is minimal in computational time, based on other performance measures CERVI-CYTO-CNN is more accurate for current use. Furthermore,

Table 7.9 compared the performance of the proposed CERVI-CYTO-CNN model with other models for classifying single cervical cancer cell.

Table 7.9 Comparison Performance of DCNN-ReLU Model for Single Cell

Methods	Accuracy %	Precision %	Recall %	F1 score %
ResNet50V2	90	70	71	73
AlexNet	91	71	78	72
DLNN	92.3	73	78.6	75.5
RVDLNN(CERVI-CYTO-NET)	92.73	71.15	88.10	78.72
DBN	95	76.5	82.5	79
RBM-DBN(CERVI-CYTO-RBM)	95.27	95.86	79.59	85.71
DCNN(CERVI-CYTO-CNN)	96.73	95.24	85.11	89.89

The table demonstrates that the proposed DCNN for single cells attained higher values than other models. The figure 7.41 represents the comparative analysis of a single cell for cancer cell classification.

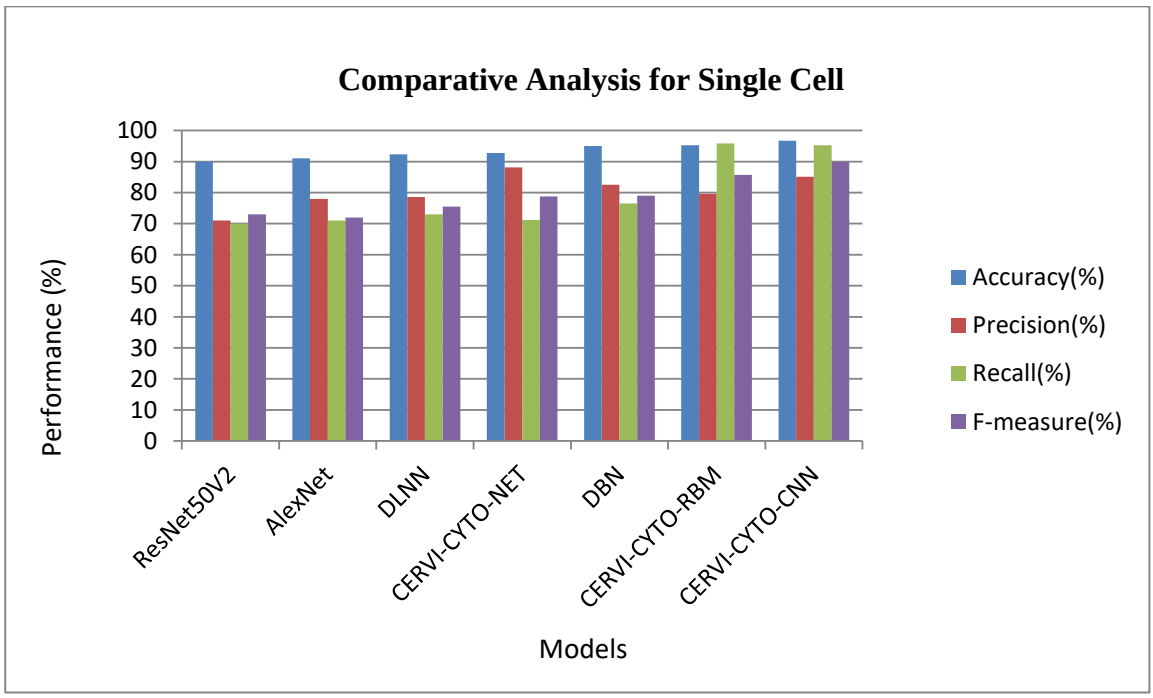

Figure 7.41 Comparative Metrics for Single Cell

Table 7.10 deliberates the comparison performance of the proposed DCNN-ReLU Model for Multi-Cell.

Table 7.10 Comparison Performance of Proposed DCNN-ReLU Model for Multi-Cell

Methods	Accuracy(%)	Precision(%)	Recall(%)	F-measure(%)
ResNet50V2	90	70.5	72.3	73.5
AlexNet	92	78.4	72	74
DLNN	92.2	76.5	93	82.5
CERVI-CYTO-NET	93.08	82.61	97.69	85.07
DBN	95	87.5	91.5	88.2
CERVI-CYTO-RBM	95.50	87.14	93.85	90.37
CERVI-CYTO-CNN	97.23	91.30	96.92	94.03

The table depicts the performance comparison of the proposed DCNN-ReLU model where it attained 97.23% accuracy, 91.30% precision, 96.92% Recall, and 94.03% F1 score.

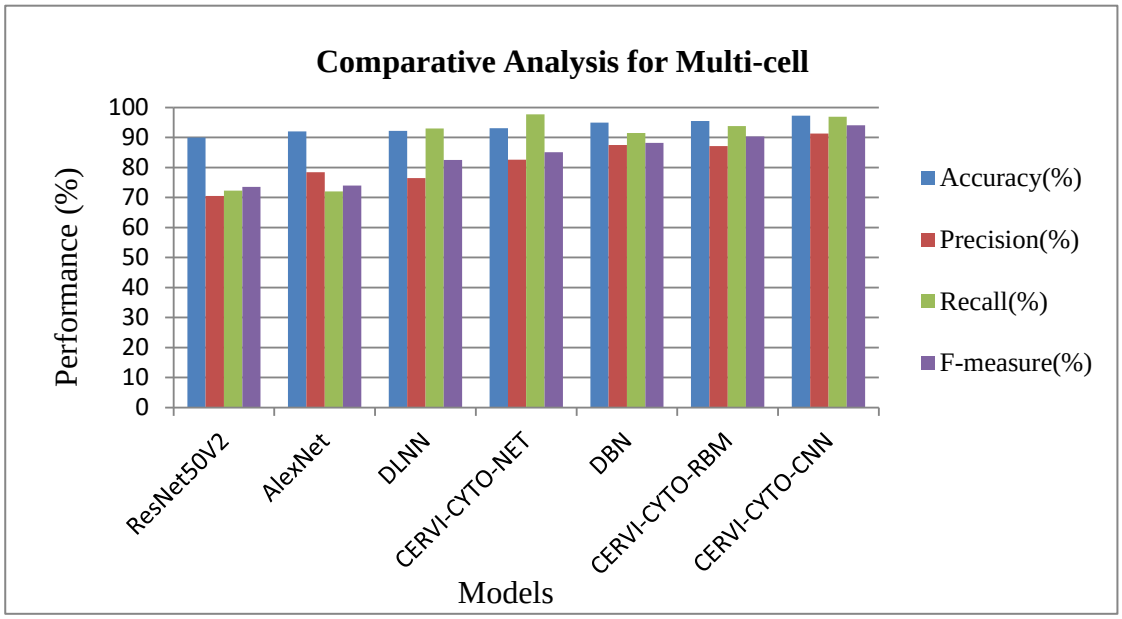

Figure 7.42 Comparison Performance of CERVI-CYTO-CNN

Figure 7.42 represents the comparison performance. In terms of accuracy, the efficiency of DCNN with ReLU outperforms ResNet50V2, AlexNet, DLNN, RVDLNN, DBN, and RBM-DBN. It attained higher accuracy, recall, precision, and F1 score than other conventional models.

7.7. Discussions and Insights

The section analyzes the results obtained and performance achieved by the proposed methods in all three models.

Cervical cancer is a hazardous illness that is one of the main reasons for the increased women prevalence rate in the world. It is necessary to identify the disease primarily in order to evade future consequences. As the traditional mechanisms involve limitations such as time-invasive processes, less efficiency, and can be prone to human error. Several traditional models utilized enormous techniques to enhance the efficacy of cervical cancer classification. Essentially, most of the existing methods focused on the diverse types of cancer such as breast cancer Desai & Shah (2021), skin cancer Shah et al. (2023), etc. However, limited studies concentrated on cervical cancer detection. To address this gap, the proposed method is intensive on cervical cancer classification. Accordingly, most of the classical systems are dedicated to single datasets Qathrady et al. (2024), but greater efficacy can be identified through the processing of multiple and diverse datasets. To resolve the issue, the presented system used two diverse datasets, the SIPaKMeD and Herlev datasets, for the classification.

Correspondingly, enormous research concentrated on various screening mechanisms such as VIA, HPV testing, and LBC for cervical precancerous lesions. In the existing method, DL based method has been used with acetic acid screening data for the classification of the pre-cancer screening model Yan et al. (2022). Similarly, classical research analyses HPV and cervical cancer Lei et al. (2022). Accordingly, DL based method has been incorporated for the screening of cervical cancer with liquid based cytology specimens Kanavati et al. (2022). In parallel, DL and transfer learning mechanisms have been designed for the detection of cervical cancer. Here, input data has been utilized from liquid-based cytology Pap smear images Wong et al. (2023). Likewise, several traditional methods focused on the diverse set of input data from various screening data.

Conversely, Pap smear test is the common screening mechanism that support in primary treatment from emerging cervical cancer. It is a significant screening mechanism utilized for the diagnosis of cervical cancer in women. Besides, it is serious for the primary identification of abnormal cell changes in the cervix, where primary identification of these cellular abnormalities assists in stopping cervical cancer development. Significantly, traditional research related to the Pap smear test on the screening of cervical cancer is limited. To tackle the issue, the presented system utilized the SIPaKMeD and Herlev datasets for cervical cancer classification. The advantages of Pap smear test are represented in the figure 7.43.

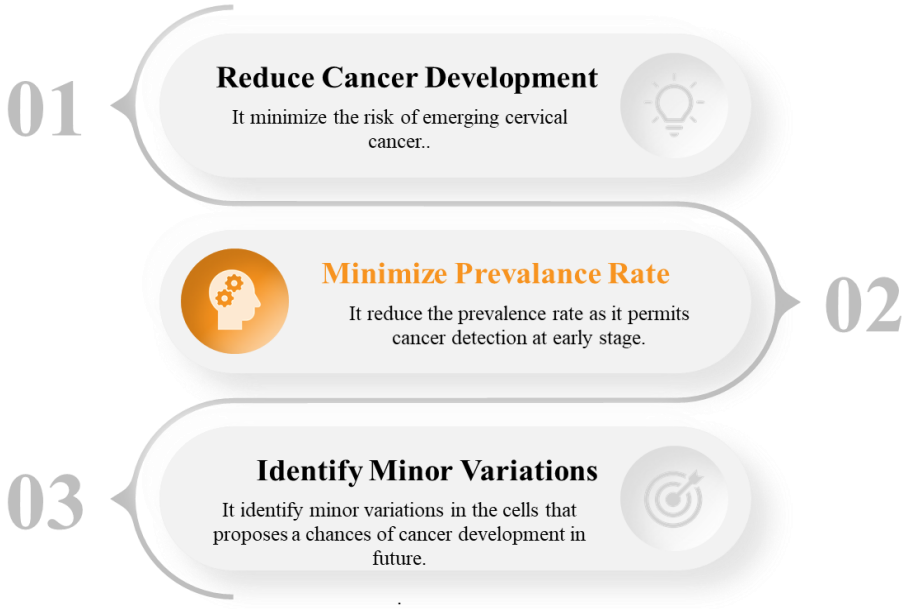

Figure 7.43 Advantages of Pap smear Test

Accordingly, several pioneering models function on the classification of cervical cancer stem cells using either single cell T. Zhang et al. (2023) or multi-cell Taneja, Ranjan, & Ujlayan (2018). The classification of both the single cell and multi-cell is important for the in-depth analysis of cervical cancer detection. To address the problem, the proposed method functions on single cell classification with the Herlev dataset and multi-cell classification with the SIPaKMeD dataset. Besides, it is identified that the classical model utilized diverse datasets for the classification of cervical cancer. Conversely, some of the classical systems are limited to handling larger datasets H. Zhang et al. (2021), which is the essential factor in determining the enhanced efficacy of the classification. To tackle the issue, the projected

method used two diverse datasets with a larger size of dataset for cervical cancer detection. The dataset comprises the normal and abnormal classes, with 917 images in the Herlev dataset and 966 images in the SIPaKMeD dataset. Correspondingly, Table 7.11 represents the limitations of the conventional system, which is resolved with the proposed approach.

Table 7.11 Comparative Analysis of Proposed Method with Classical Systems

S.No	References	Aim and Objective	Limitations	Advantages of the proposed System
1.	Gonçalves, Souza, & Fernandes (2022; Mahmood, Arsalan, Owais, Lee, & Park (2020; Rahman et al. (2023; Shah et al. (2023)	The major aim of the classical system is to detect breast cancer and skin cancer.	Several traditional approaches focused on skin cancer, breast cancer, and blood cancer. However, existing methods for cervical cancer are limited.	The proposed approach is focused on the classification of cervical cancer.
2.	Qathrady et al. (2024)	The objective of the traditional model is to detect cervical cancer.	It is lacked in the processing of multiple and diverse datasets.	The presented method used two types of datasets.
3.	Taneja et al. (2018; T. Zhang et al. (2023)	The main aim of the classical models is the identification of cervical cancer stem cells and Multi-cell nuclei segmentation in cervical cancer images.	The drawbacks of the traditional method are that it is limited by functioning on either a single cell or multi-cell classification.	The projected system is focused on both singe cell and multi cell classification.

4.	H. Zhang et al. (2021)	The chief objective of the classical system is early diagnosis of cervical cancer.	The limitation of the classical model is the handling of larger datasets.	The respective research utilized two diverse datasets, with 917 images in the Herlev dataset and 966 images in the SIPaKMeD dataset.
5.	Kanavati et al. (2022; Lei et al. (2022; Yan et al. (2022)	The foremost goal of the conventional systems is cervical cancer screening analysis.	Traditional research focused on liquid-based cytology specimens, acetic acid screening data, and HPV data. However, traditional models limit pap smear data.	The proposed approach used pap smear data for cervical cancer screening.
6.	Ilyas & Ahmad (2021)[13]	The main aim of the existing method is cervical cancer screening	It is limited through lower accuracy and efficacy	The presented model attained higher accuracy and efficacy which is verified over comparative analysis outcomes.

Correspondingly, in the performance metrics, accuracy is the significant metric utilized to reveal the model's efficacy. However, enormous traditional methods are limited through metric accuracy. In the classical approach, the SMOTE algorithm and genetic algorithm are processed in cervical cancer screening with an accuracy value of 94% Newaz, Muhtadi, & Haq (2022). Similarly, ResNet101and SVM based system has been utilized for the classification of cervical cancer with an accuracy of 92% Alquran et al. (2022). Likewise, several traditional systems attempted to attain better efficacy in cervical cancer but were limited through accuracy metrics Ilyas & Ahmad (2021), Huang et al. (2020; Priyanka (2021;

Qathrady et al. (2024). To resolve the issue, the proposed method with three models attained an accuracy value of 95.51% in model 2 and 97.23% in model 3. It is significantly higher than the classical systems, which show greater performance of the presented methods. Figure 7.44 represents the accuracy value of the proposed models and accuracy percentage is shown in Table 7.12.

Table 7.12 Accuracy Analysis of Proposed Models

Models	Accuracy %
CERVI-CYTO-NET	Single cell- 92.73% Multi cell –93.08%
CERVI-CYTO- RBM	Single cell- 95.27% Multi cell- 95.50%
CERVI-CYTO-CNN	Single cell – 96.7% Multi-cell - 97.23%

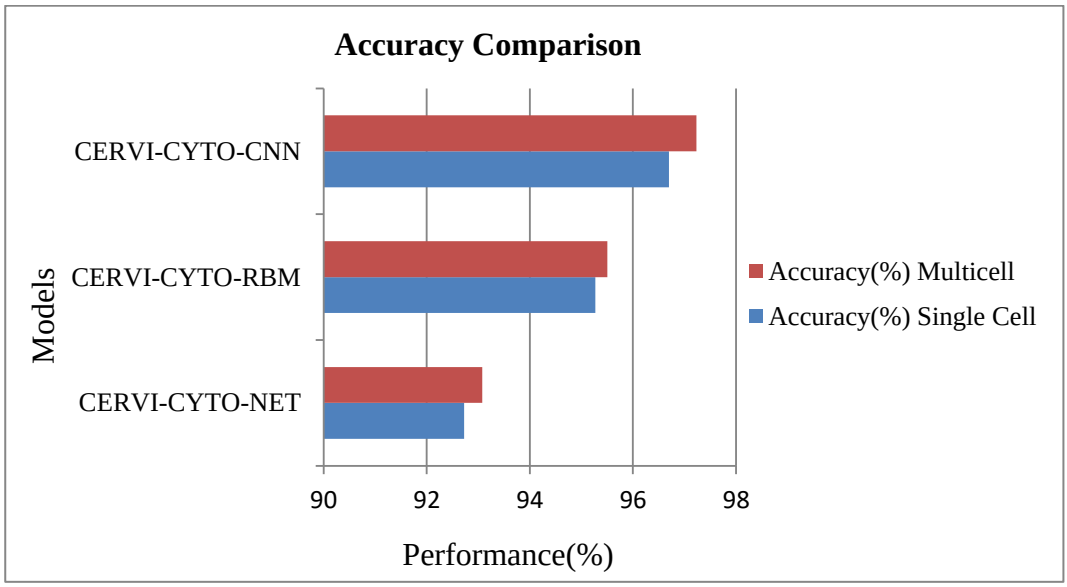

Figure 7.44 Accuracy of the Proposed Models

The accuracy obtained by the classifiers highly influences the overall diagnosis. In a medical setting, this could 90% accuracy means that 1 in 10 patients might receive an incorrect diagnosis. The accuracy percentile may be acceptable in scenarios where the cost of a false negative (missing a case of cancer) is mitigated by additional testing or where the prevalent criteria are low. However, it still necessitates careful consideration of the potential

risks and benefits. When the accuracy is 94% it indicates a more reliable model, with only 4% of cases potentially being misclassified. This can lead to greater confidence in the model's predictions and might reduce the need for additional confirmatory tests. It could also mean fewer false positives, which can help avoid unnecessary treatments or anxiety for patients.

Even though classification accuracy plays a vital role in estimating the performance of a classifier, yet there are several other factors influencing the usage of a system in real-time. It includes the dataset or number of images utilized for training and testing the model, the values of false positives and false negatives, computational time etc.

The presented system in Model 1 utilized the advantages of the RVDLNN classifier, model 2 used the advantages of the RBM-DBN classifier, and Model 3 used the advantages of the DCNN classifier to attain greater performance in the classification of normal and abnormal cervical cells for the detection of cervical cancer screening which is verified over the results. The three models developed here are connected with other. Model 2 is an enhanced version of Model 1. Meanwhile, Model 3 is the enhanced version of Model 2. Developing and comparing different techniques in various models can be beneficial in understanding the capability of various techniques thus contributing for future research in the field. Here Model 2 extracts more features than Model 1 which can help in better understanding of the image. Moreover, higher performance is acquired with significant benefits, which is indicated in the following:

- The proposed approach is intensely focused on the classification of cervical cancer from Pap smear images.
- The presented models used two types of datasets for the classification of cervical cancer utilizing both single cell and multi-cell images.
- The single cell dataset, Herlev dataset contains 917 single cell images and the SIPaKMeD dataset contains 966 multi-cell images.
- The proposed models assist in the primary screening of cervical cancer which is helpful for the lab technicians and the physicians for initial analysis. It can reduce the analysis time by avoiding the cells that do not need further examination. Thus the waiting time for results can be reduced thus helping the further process easier for the women.

- The results of the research shows that greater accuracy, better noise handling, higher efficacy and the models also are capable of handling over-fitting of data compared to the traditional models.

7.8. Summary

In the chapter 7, details about the results obtained for the three proposed models are shown. This chapter explains the results of three models CERVI-CYTO-NET, CERVI-CYTO-RBM, and CERVI-CYTO-CNN based on accuracy, precision, recall, and F-measure and also the comparison of the proposed models with other existing models are shown based on the results. The results illustrate that the proposed models are performing better than the existing models and the CERVI-CYTO-CNN model gives the best performance among the three.